indicate that after the first day of culture the pLRF released was newly synthesized. These findings are consistent with previous studies showing that placental tissue in vitro releases its initial content of immunoreactive LRF during the first 24 hours of culture (*3*).

The remaining eluates of pLRF from the CM-cellulose chromatography were pooled and concentrated by Diaflo filtration. The pLRF of the resulting concentrate was measured by radioimmunoassay and doses of 1.5, 2.0, 5.0, 7.0, and 9.3 ng were injected intravenously into five adult male rats. An increase in LH release was observed. Similar doses of synthetic LRF were injected into another group of male rats and this elicited an LH response similar to that of the pLRF. The total net increase of LH (minus the baseline) was calculated from 0 to 60 minutes after the injection of either pLRF or synthetic LRF. Linear regression analysis of the total net LH release stimulated by similar doses of pLRF and synthetic LRF yielded a correlation coefficient of .944 ($P < .002$). Thus the pLRF obtained by CM-cellulose chromatography was biologically equipotent to synthetic LRF.

This study demonstrates that the human placenta synthesizes a pLRF that is immunologically, physiochemically, and biologically indistinguishable from hypothalamic LRF. We have postulated that the function of this pLRF may be to control hCG secretion and thus may affect steroidogenesis during pregnancy. We demonstrated previously that synthetic LRF can stimulate α- and β-hCG release by the human placenta in vitro and that the stimulation of β-hCG occurs in a dose-response manner (*2, 5*); these findings were confirmed by other investigators, as was the stimulation of adenosine 3′,5′-monophosphate production by synthetic LRF (*6*). Recently, we found that circulating chorionic gonadotropin in the pregnant monkey increased after the administration of synthetic LRF (*7*). The amino acid sequence, chemical nature, and biological significance of the pLRF synthesized by the placenta remain to be determined.

G. S. KHODR
T. M. SILER-KHODR
Department of Obstetrics and Gynecology, University of Texas Health Science Center, San Antonio 78284

References and Notes

1. R. Burgess *et al.*, *Proc. Natl. Acad. Sci. U.S.A.* **69**, 178 (1972); S. S. C. Yen *et al.*, *J. Clin. Endocrinol. Metab.* **33**, 882 (1971).
2. T. M. Siler-Khodr and G. S. Khodr, *Am. J. Obstet. Gynecol.* **130**, 216 (1978); G. S. Khodr and T. M. Siler-Khodr, *Fertil. Steril.* **29**, 523 (1978); *Endocrinology* **100**, A354 (1977); 25th Annual Meeting of the Society for Gynecologic Investigation, Atlanta (1978), abstr. 3, p. 2.
3. T. M. Siler-Khodr and G. S. Khodr, *Fertil. Steril.*, in press.
4. R. H. Asch, E. O. Fernandez, T. M. Siler-Khodr, C. J. Pauerstein, *Am. J. Obstet. Gynecol.*, in press.
5. G. S. Khodr and T. M. Siler-Khodr, *Fertil. Steril.* **30**, 301 (1978); 26th Annual Meeting of the Society for Gynecologic Investigation, San Diego (1979), abstr. 141, p. 85.
6. S. Miura, R. Osathanondh, A. Markis, R. B. Todd, L. A. Levesque, K. J. Ryan, 26th Annual Meeting of the Society for Gynecologic Investigation, San Diego (1979), abstr. 168, p. 102.
7. T. M. Siler-Khodr, G. S. Khodr, C. Eddy, C. J. Pauerstein, *Endocrinology* **104**, 199A (1979).
8. This work was supported in part by institutional grants 801 RR05654 and 8-08 and NIH grant 5 P30 HD10202. Reagents for the α-hCG and hCS radioimmunoassays were supplied by the NIAMDD and for the β-hCG by V. Stevens. Standard IS-2-hCG was provided by the WHO. We thank G. Cadena, J. Rhode, P. Koym, and L. Chadwell for technical assistance and G. Small for secretarial assistance.

29 May 1979; revised 22 October 1979

Toward a Functional Architecture of the Retina: Serial Reconstruction of Adjacent Ganglion Cells

Abstract. *Twenty adjacent ganglion cells in cat retina were partially reconstructed from electron micrographs of serial thin sections. Cells were classified by size and by dendritic branching patterns as α, β, or γ cells. The α and β cells were further subdivided by differences in the laminar distribution of their dendrites in the inner plexiform layer. The distribution of synaptic contacts on the cells was distinctive for each of the five major classes. Contacts on the α and β cells were mainly on the dendrites in the sublamina in which a cell's major dendritic arborization was contained.*

There has been substantial progress in correlating the anatomical structure of cat retinal ganglion cells with their electrophysiological properties. Based on Golgi impregnations of single neurons, Boycott and Wässle (*1*) divided the ganglion cell population into α cells (large somas and broad, radiate dendritic trees), β cells (medium-sized somas and narrower, bushy dendritic trees), and γ cells (small somas, varied dendritic geometry). [The α, β, and γ cells seem to correspond to Y, X, and W cells, respectively, in the current physiological scheme (*2*).] Ganglion cells have been further subdivided anatomically according to the height in the inner plexiform layer (IPL) at which their dendrites arborize. Cells that branch in the outer third of the IPL have off-center receptive fields, whereas cells that branch in the inner two-thirds of the IPL have on-center receptive fields (*3*).

Table 1. Diameter, surface area, and volume for each of 20 reconstructed ganglion cell bodies. Differences in surface area and volume for somas of the same diameter reflect differences in shape.

Size category	Diameter (μm)	Surface area (μm^2)	Volume (μm^3)
α	> 31*	1,705	10,049
	> 25*	1,654	9,250
β	19	1,117	4,532
	19	1,032	4,120
	18	855	2,931
	17	937	3,475
	16	855	2,957
	16	757	3,558
	15	931	2,956
γ	12	123	934
	12	434	1,085
	10	564	1,261
	10	337	671
	9	242	468
	9	347	713
	9	350	547
	8	165	338
	8	166	222
	7	162	221
	6	158	211

*Minimum value; cell did not reach its maximum diameter within series.

Little is known about the distribution of synaptic contacts on ganglion cells. We lack such basic information as whether the contacts are on the cell bodies or the primary dendritic shafts, and whether [as the data of Nelson *et al.* (*3*) would suggest] the contacts are restricted to the dendritic branches in the sublamina of each cell's major arborization. Nor is much known about the biophysically relevant parameters for each cell type, such as soma surface area. The latter is particularly important, since it can be a major determinant of a cell's input impedance (*4*). Finally, the distribution of the five cell classes within a small patch of retina is unknown because the Golgi method, which defines each class by soma size and branching pattern, stains only a few of the neurons in a given region.

Reconstruction from electron micrographs permits study of the microdistribution, dendritic and synaptic patterns, and biophysically relevant parameters of specific ganglion cell types. We have begun to gather such information by partially reconstructing a group of adjacent ganglion cells from 150 serial sections photographed with the electron microscope. The series encompassed a block of tissue (about 15 by 150 by 200 μm) taken from within 1° to 2° of the area

0036-8075/80/0118-0317$00.50/0

centralis (5). The photographed region contained major portions (60 percent or more) of the cell bodies of 20 ganglion cells. Each soma was reconstructed (6), and its flat-mount diameter and surface area were estimated (7). For 14 cells we reconstructed as much of the dendritic tree and associated synaptic contacts (6) as was present in the series. Enough detail was obtained to match each cell with one of the five classes established by light microscopy and to suggest that each class may have a distinctive pattern of synaptic contacts.

The 20 reconstructed somas formed three distinct size classes (Table 1). Two large (α) neurons (10 percent of the sample) had flat-mount diameters of at least 25 and 31 μm and soma surface areas of at least 1600 μm^2. Seven medium-sized (β) neurons (35 percent of the sample) had flat-mount diameters of 15 to 19 μm and surface areas of 931 to 1117 μm^2. Eleven small (γ) neurons (55 percent of the sample) had flat-mount diameters of 6 to 12 μm and surface areas of 123 to 564 μm^2. The cell volumes also sorted into the same distinct groups. The idea that, within a particular retinal region, the size distribution of ganglion cell somas is trimodal seems well supported by these findings, although, on the basis of the sample size, we would not insist that the groups do not overlap.

The dendrites of the α cells (Fig. 1A) were stout with pale cytoplasm and meandered through the IPL without major bifurcation. In contrast, the dendrites of the β cells (Fig. 1B) had dark cytoplasm and branched repeatedly within the reconstructed region. (The association of dark dendritic cytoplasm with β cells and pale dendritic cytoplasm with α cells was observed in several additional retinas.) For each of the five β cells, the dendritic tree could be traced to tertiary and, in some cases, quaternary, branches. The processes of the γ cells (Fig. 1C) were not so easily characterized; several gave rise to fine dendrites that traveled some distance without branching, while others gave rise to a major stalk that subdivided almost immediately. These variations were not surprising, since Boycott and Wässle (1) and Cajal (8) have described the small cells as a rather heterogeneous group.

Differences between cells in the laminar distribution of their dendrites were recognizable in the reconstructions and could be used to further subdivide the cells. Thus the α cell on the left in Fig. 1A sent its primary dendrite directly to the outer third of the IPL, whereas the α cell on the right maintained its dendrites over a comparable distance in the inner third of the IPL. Similarly, two β cells each had a single stout primary dendrite that reached sublamina *a* before subdividing into tertiary or quaternary branches, whereas three other β cells confined most of their dendritic branches to the middle third of the IPL. Dendrites of γ cells branched only in the inner and middle thirds of the IPL. However, Kolb (9) reconstructed what appears to be a γ cell with its major arborization in the outer third of the IPL.

The distribution of synaptic contacts was characteristic for the α and β cell classes and was matched to their major patterns of dendritic arborization (Fig. 1, A and B). For example, the α cell on the left in Fig. 1A had no contacts on its soma or the proximal portion of its dendrite, but received numerous contacts once the dendrite reached the outer third of the IPL. The other α cell received numerous contacts proximally on all three of its primary dendrites. Similarly, β cells had few contacts on their somas or the proximal portions of their dendrites, but when the dendrites reached the height in the IPL at which subdivision began in earnest, the number of synaptic contacts increased sharply. The pattern of synaptic contact on γ cells was varied. Several had substantial numbers of somatic contacts, whereas others, following the pattern seen in α and β cells, had few contacts on the soma or proximal dendrites and relatively more contacts in the regions of major branching.

Much of the information on a cell's intrinsic properties (such as size, shape, and pattern of branching) could previously be gathered only from neurons stained in isolation. In our study, such information was gathered from adjacent cells. The reconstructed dendritic arborizations were less complete than one is used to from Golgi material, partly because the series spanned a thickness of only 15 μm (compared to 100 μm for a typical Golgi section); therefore some dendrites—particularly those of α cells—extended out of the plane of the series and were lost. However, the reconstructions were more complete than they seem. Close to the area centralis, from which the present series was taken, the dendritic field diameters are actually quite small,

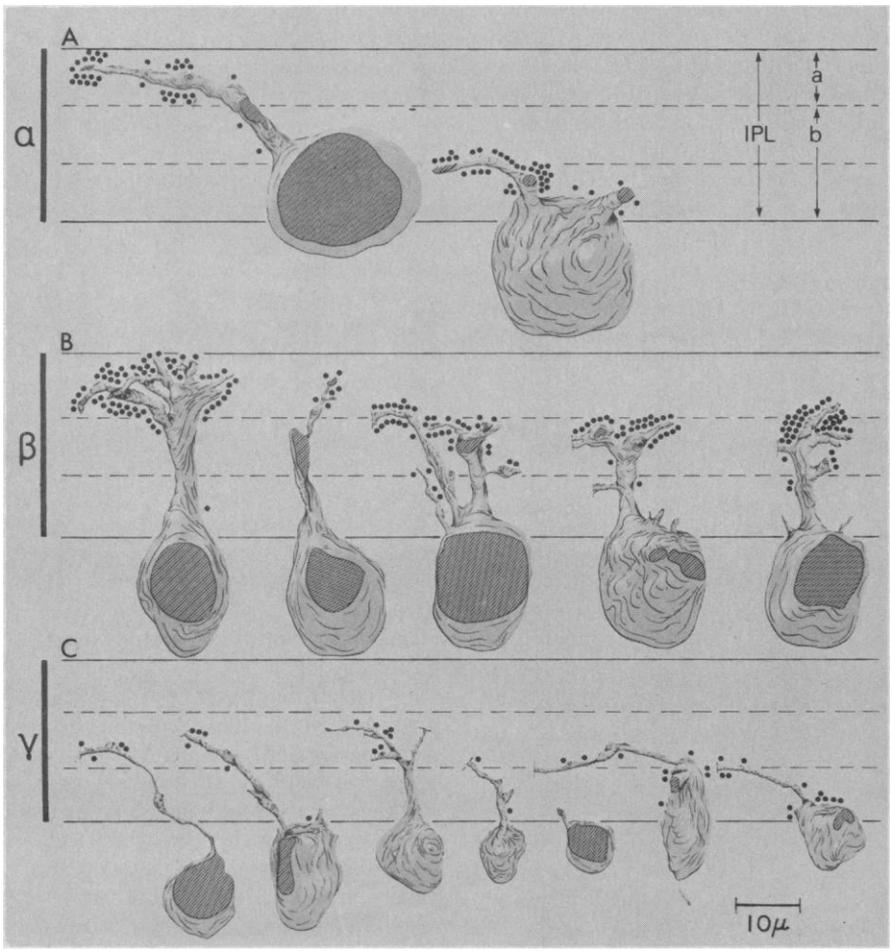

Fig. 1. Reconstructions of 14 ganglion cells from electron micrographs of 150 serial sections. Sublaminae *a* and *b* of the IPL are indicated by arrows. Black dots represent synaptic contacts. Cross-hatching indicates portion of cell missing from the series.

the lower limit from Golgi observations being only 20 μm for β cells and 180 μm for α cells (*1*). The field diameters of some of the reconstructed dendrites were not so far from this: dendritic field diameters of two reconstructed β cells reached 25 and 28 μm, and that of a reconstructed α cell reached 50 μm. Most encouraging, the reconstructions provided more than enough detail for recognizing, at the electron microscopic level, soma sizes and the patterns and laminar distributions of dendrites described with light microscopy. The fact that each of the reconstructed neurons could be placed in one of the five major categories of ganglion cells means that the microdistribution of ganglion cells can now be studied in a systematic manner.

The greatest reward of the reconstructions was that they revealed the distribution of synaptic contacts on each cell. It was surprising to find, for example, that the α and β cells had few contacts on their somas and that the contacts on the dendrites of a particular cell tended to be restricted to the IPL sublamina in which its major arborization was contained. The distribution of synaptic contacts seems to be specific for each class, supporting the overall classification scheme. These findings also support and extend similar work by Kolb (*9*).

The next tasks are to identify the sources of the synaptic contacts by tracing them through a series of sections back to their cells of origin, to identify the transmitter chemistry of these presynaptic elements, and to analyze the cable properties of the ganglion cells and their inputs in order to understand the effects of the different soma surface areas and dendritic geometries. Contributions toward these ends made with the reconstruction approach are presented elsewhere (*10*).

JOHN K. STEVENS*
Department of Physiology, University of Pennsylvania School of Medicine, Philadelphia 19104
BARBARA A. MCGUIRE
PETER STERLING
Department of Anatomy, University of Pennsylvania School of Medicine

References and Notes

1. B. B. Boycott and H. Wässle, *J. Physiol. (London)* **240**, 397 (1974). See also A. Hughes, J. Stone, Y. Fukuda [*J. Neurophysiol.* **37**, 722 (1974)], and A. Hughes [*J. Comp. Neurol.* **163**, 107 (1975)].
2. C. Enroth-Cugell and J. Robson, *J. Physiol. (London)* **187**, 517 (1966); B. G. Cleland, M. W. Dubin, W. R. Levick, *ibid.* **217**, 473 (1971); Y. Fukuda, *Vision Res.* **11**, 209 (1971); J. Stone and K.-P. Hoffman, *Brain Res.* **43**, 610 (1972); J. K. Stevens and G. L. Gerstein, *J. Neurophysiol.* **39**, 213 (1976).
3. R. Nelson, E. V. Famiglietti, H. Kolb, *J. Neurophysiol.* **41**, 472 (1978).
4. W. Rall, *ibid.* **30**, 1138 (1967); O. F. Schanne and E. P. Ceretti, *Impedance Measurements in Biological Cells* (Wiley, New York, 1978); J. N. Barrett and W. E. Crill, *J. Physiol. (London)* **239**, 301 (1974); *ibid.*, p. 325; H. D. Lux, P. Schubert, G. W. Kreutzberg, in *Excitory Synaptic Mechanisms*, P. Anderson and J. K. S. Jansen, Eds. (Universitetsforlaget, Olso, 1970), p. 189.
5. The retina was taken from an adult cat perfused with buffered aldehydes and was prepared for electron microscopy in the standard manner. Silver-gold sections (100 nm) were stained with uranium and lead. We determined that the block was within 1° to 2° of the area centralis by comparing the density of ganglion cells prepared from a series of 2-μm sections that passed completely through the area centralis.
6. Two overlapping electron micrographs were made of each section at ×1300, the lowest magnification adequate for resolving synaptic contacts. A cell was reconstructed by tracing its outline from successive prints (final magnification, ×3400) onto separate acetate sheets and, using appropriate fiducial marks, aligning the sheets on a cartoonist's jig. Synaptic contacts were identified by viewing the prints through a dissecting microscope at a maximum magnification of ×120,000. Contacts were defined as sites of vesicle accumulation associated with a presynaptic ribbon or with increased density of presynaptic and postsynaptic membranes.
7. We chose the profile in which the cell's cross-sectional area was greatest and divided it by a series of 30 to 50 chords that were parallel to the retinal surface and orthogonal to the plane of section; the longest chord approximated the flat-mount diameter. An equivalent cylinder was generated for each chord; the sum of their surface areas and the sum of their volumes provided estimates of the soma surface area and volume, respectively. Although the values are given in micrometers (Table 1), shrinkage makes them less than the actual values.
8. S. Ramon y Cajal, *The Structure of the Retina*, compiled and translated by S. A. Thorpe and M. Glickstein (Thomas, Springfield, Ill., 1972).
9. H. Kolb, *J. Neurocytol.* **8**, 295 (1979).
10. S. Ellias and J. K. Stevens, in preparation; Y. Nakamura, B. A. McGuire, P. Sterling, *Proc. Natl. Acad. Sci. U.S.A.*, in press.
11. Supported by National Eye Institute grants EY00828, EY01832, and EY01583. We thank D. Netsky and T. Davis for their help, B. Woolsey and J. Woolsey for their artistic rendering of the reconstructions, and H. Abriss for typing the manuscript. We are particularly indebted to F. Letterio and E. Shalna for their technical support.
* Present address: PlayFair Neuroscience Unit, Toronto Western Hospital, Toronto, Ontario, Canada M5T 2S8.

19 September 1979; revised 25 October 1979

Reduction of the Isoproterenol-Induced Alterations in Cardiac Adenine Nucleotides and Morphology by Ribose

Abstract. *Continuous intravenous infusion of ribose (200 milligrams per kilogram per hour) for 24 hours induced a marked stimulation of cardiac adenine nucleotide biosynthesis in unanesthetized and unrestrained rats that had been treated with isoproterenol subcutaneously (25 milligrams per kilogram). The diminution of adenine nucleotides characteristic for the action of high doses of isoproterenol was entirely prevented, and the incidence of the isoproterenol-induced myocardial cell damage was significantly reduced when ribose was administered. These results support the view that depletion of adenine nucleotides is involved in the development of cardiac necrosis.*

Isoproterenol, a synthetic catecholamine, is well known for its pronounced positive inotropic effect mediated by an increased transmembrane Ca^{2+}-influx into the myocardial cell (*1*, *2*). Because of an excessive consumption of adenosine triphosphate (ATP), the cardiac adenine nucleotide pool becomes diminished under these conditions (*1*, *3*). It is this ATP decrease that has been considered responsible for the development of myocardial cell lesions (*3*) occurring after application of high doses of isoproterenol in rats (*4*). Various attempts have been made to prevent or reduce the isoproterenol-induced cardiac cell damage, including administration of high potassium and low sodium diets (*5*), application of β-receptor-blocking agents (*6*), and treatment with calcium-antagonistic compounds and calcitonin, and acidification (*3*). These interventions tend to attenuate the positive inotropic effect of isoproterenol and to prevent the diminution of cardiac ATP, thus maintaining the structural integrity of the myocardium.

Table 1. Concentrations of ATP and of adenine nucleotides (AN; sum of ATP, ADP, AMP) and rates of AN biosynthesis in the myocardium of rats under control conditions and 24 hours after subcutaneous application of isoproterenol (25 mg/kg), with constant intravenous infusion of either 0.9 percent NaCl or ribose (200 mg/kg per hour) for 24 hours. Results are given as mean values ± the standard error of the mean; the numbers in parentheses indicate the number of experiments.

Isoproterenol addition	ATP (nmole/g)	AN (nmole/g)	AN change after isoproterenol (nmole/g per 24 hours)	Biosynthesis of AN (nmole/g per 24 hours)
None	4470 ± 84 (34)	5893 ± 103 (34)		6.0 ± 0.7 (25)
NaCl	3167 ± 62* (9)	4190 ± 84* (9)	−1703	22.5 ± 3.7* (4)
Ribose	4565 ± 292 (6)	6047 ± 208 (6)		80.1 ± 11.1* (8)

*$P < .005$ compared with the control values

0036-8075/80/0118-0319$00.50/0